

The Effects of Relativistic Corrections on Cosmological Parameter Estimations from SZE Cluster Surveys

Zuhui Fan^{1,2} and Yanling Wu¹

ABSTRACT

Sunyaev-Zel'dovich Effect (SZE) cluster surveys are anticipated to yield tight constraints on cosmological parameters such as the equation of state of dark energy. In this paper, we study the impact of relativistic corrections of the thermal SZE on the cluster number counts expected from a cosmological model and thus, assuming that other cosmological parameters are known to high accuracies, on the determination of the w parameter and σ_8 from a SZE cluster survey, where $w = p/\rho$ with p the pressure and ρ the density of dark energy, and σ_8 is the rms of the extrapolated linear density fluctuation smoothed over $8 \text{ Mpc} h^{-1}$. For the purpose of illustrating the effects of relativistic corrections, our analyses mainly focus on $\nu = 353 \text{ GHz}$ and $S_{lim} = 30 \text{ mJy}$, where ν and S_{lim} are the observing frequency and the flux limit of a survey, respectively. These observing parameters are relevant to the *Planck* survey. It is found that from two measurable quantities, the total number of SZE clusters and the number of clusters with redshift $z \geq 0.5$, σ_8 and w can be determined to a level of $\pm 1\%$ and $\pm 8\%$, respectively, with 1σ uncertainties from a survey of 10000 deg^2 . Relativistic effects are important in determining the central values of σ_8 and w . If we choose the two quantities calculated relativistically from the flat cosmological model with $\sigma_8 = 0.8284$ and $w = -0.75$ as input, the derived σ_8 and w would be 0.819 and -0.81 , respectively, if relativistic effects are wrongly neglected. The location of the resulting σ_8 and w in the $\sigma_8 - w$ plane is outside the 3σ region around the real central σ_8 and w .

Subject headings: cosmology: theory— galaxy: cluster — large-scale structure of universe

¹Department of Astronomy, Peking University, Beijing 100871, China

²Beijing Astrophysics Center, Chinese Academy of Science and Peking University, Beijing 100871, China

1. Introduction

With fast advances in astronomical observations, the determination of cosmological parameters has become one of the most important studies in cosmology (e.g., Eisenstein, Hu & Tegmark 1999; Spergel et al. 2003). Different kinds of observables are sensitive to different underlying physical processes, and thus can be used to probe different cosmological parameters. The local abundance and the evolution of clusters of galaxies have been used extensively in the Ω_m and σ_8 determination, where Ω_m is the present matter density parameter of the universe and σ_8 is the rms of the extrapolated linear density fluctuation smoothed over $8 \text{ Mpc} h^{-1}$ (e.g., Bahcall & Fan 1998; Pen 1998; Haiman, Mohr & Holder 2001; Holder, Haiman & Mohr 2001; Fan & Chiueh 2001; Rosati, Borgani & Norman 2002). Supernova type Ia (SNeIa) (Schmidt et al. 1998; Perlmutter et al. 1999) and Cosmic Microwave Background (CMB) radiation observations (e.g., Spergel et al. 2003) provide convincing evidences that we are living in a flat universe with about 70% of the matter being in the form of dark energy. As the properties of dark energy affect the global geometry of the universe and the growth of matter density fluctuations, the abundance and the evolution of clusters are dependent of the w parameter of the equation of state of dark energy, where $w = p/\rho$ with p the pressure and ρ the density of dark energy (e.g., Caldwell, Dave, & Steinhardt 1998). Studies show that deep and large cluster surveys could constrain w to about 5% level (e.g., Mohr et al. 2002). In order to reach such a precision, however, we have to understand different types of systematic effects. Investigations indicate that the incompleteness of the knowledge about the intracluster gas (ICM) affects the cosmological parameter determination from X-ray cluster surveys, but influences less on the results from Sunyaev-Zel'dovich Effect (SZE) cluster surveys (Majumdar & Mohr 2003). In this paper, we study the impact of relativistic corrections of thermal SZE on the w and σ_8 estimation from SZE cluster surveys.

The typical gas temperature in clusters of galaxies is about a few keV, but clusters with temperatures as high as about 17 keV have been observed (e.g., Pointecouteau et al. 1999; 2001). Thus relativistic corrections on SZE can be significant (e.g., Birkinshaw 1999; Carlstrom, Holder & Reese 2002; Rephaeli 2002). For a SZE cluster survey, the selection function is mostly related to a mass threshold that depends on the sensitivity of the instrument and is also a function of redshift. For a survey with a relatively high flux limit, only clusters with large masses, and therefore high temperatures, can be detected. In this case, we expect that relativistic corrections will impact the theoretical estimations of the survey results considerably. The amplitude of the change of SZE due to relativistic effects also depends on observing frequencies, with a relatively large correction around 400 GHz. For *Planck*, one of the best frequencies for SZE observation is 353 GHz and the flux limit is about 30 mJy (e.g., Diego et al. 2002). Both numbers indicate that we need to take relativistic effects into account in relating cosmological models to survey results. Diego, Hansen & Silk (2003)

discussed how the corrections affect the extraction of SZE signals from *Planck* survey. Here we study the impact on the SZE cluster number counts for different w models. Keeping other cosmological parameters fixed, we particularly investigate the influence on the w and σ_8 determination.

For the redshift distribution of SZE clusters, the differences of different w models mainly show up at high redshifts. To extract w and σ_8 , we then propose to use the total number of SZE clusters N_{tot} and the number of clusters with redshift $z \geq z_m$ (denoted as $N_{z \geq z_m}$) as constraints, where z_m is flux dependent. Thus to apply our method, one needs to know the redshift range of a cluster, but not its exact value. Therefore it provides an economic way to estimate cosmological parameters from large surveys, such as *Planck*.

To demonstrate relativistic effects clearly, we consider single-frequency measurements with $\nu = 353$ GHz and the flux limit $S_{lim} = 30$ mJy. Real *Planck* observations will be multi-frequency. Therefore for a particular cluster-detecting method, realistic simulations including survey characteristics are needed to quantify carefully the influence of relativistic corrections. More discussions on this regard are presented in Section 4.

Our study finds that for a survey of 10000 deg^2 , σ_8 can be constrained to a narrow range with about $\pm 1\%$ accuracy around its central value if 1σ uncertainties are allowed for both N_{tot} and $N_{z \geq 0.5}$. The corresponding range for w is $\pm 8\%$. Relativistic effects are significant in terms of locating the central values of cosmological parameters. If they are ignored in deriving σ_8 and w from the observed N_{tot} and $N_{z \geq 0.5}$, the misplaced location of (σ_8, w) in $\sigma_8 - w$ plane is outside the 3σ region around the real central ones.

The paper is organized as follows. Section 2 contains the relevant analytical formulation. Section 3 presents numerical results. Discussions are made in Section 4.

2. Formulation

2.1. Thermal SZE with Relativistic Corrections Included

The thermal SZE, i.e., the thermal distortion of the CMB spectrum, is generated through the scattering of CMB photons with thermalized hot electrons in, e.g., clusters of galaxies (e.g., Sunyaev & Zel'dovich 1980; Birkinshaw 1999; Carlstrom, Holder & Reese 2002). Because the temperature of electrons is generally much higher than that of the CMB photons, inverse Compton scatterings are dominant, and the distribution of photons shifts toward high-frequency side. In terms of the dimensionless quantity $x = h_p \nu / k_B T_{CMB}$, where h_p and k_B are the Planck's constant and the Boltzmann's constant, respectively, and ν and T_{CMB}

are, respectively, the frequency and the temperature of CMB photons, in the nonrelativistic limit, the change of the CMB intensity can be written as

$$\frac{\Delta I}{I_0} = Q(x)y, \quad (1)$$

where $I_0 = (2h_p/c^2)(k_B T_{CMB})^3/h_p^3$,

$$Q(x) = \frac{x^4 e^x}{(e^x - 1)^2} \left[\frac{x}{\tanh(x/2)} - 4 \right],$$

and the Compton y-parameter

$$y = \int n_e \sigma_T \left(\frac{k_B T_{gas}}{m_e c^2} \right) dl,$$

where n_e is the number density of hot electrons, σ_T is the Thomson cross section, T_{gas} is the intracluster gas temperature, m_e is the electron mass, and c is the speed of light. The integral is along the line of sight.

In this limit, the shape of the distortion is independent of the gas temperature. For $\nu < 218$ GHz, $Q(x) < 0$, and the SZE shows as an absorber (or decrement) of CMB. For $\nu > 218$ GHz, $Q(x) > 0$, and the SZE shows as a source (increment) of radiation.

For relativistic corrections, we use the analytical formula of Itoh, Kohyama & Nozawa (1998), which includes terms up to $(k_B T_{gas}/m_e c^2)^5$. Then we have

$$\frac{\Delta I}{I_0} = \frac{yx^4 e^x}{(e^x - 1)^2} (Y_0 + \theta_e Y_1 + \theta_e^2 Y_2 + \theta_e^3 Y_3 + \theta_e^4 Y_4), \quad (2)$$

where $\theta_e = k_B T_{gas}/(m_e c^2)$ and

$$Y_0 = \frac{x}{\tanh(x/2)} - 4,$$

and Y_1 , Y_2 , Y_3 and Y_4 are complicated functions of x [see Itoh et al. (1998) for detailed expressions].

In Figure 1 we show the single-scattering $\Delta I/I_0$ for $k_B T_{gas} = 5$ keV and for $k_B T_{gas} = 20$ keV. For each pair, the solid and the dashed lines are the results without and with relativistic corrections, respectively. It is seen that the effects are significant for $k_B T_{gas} = 20$ keV, with about 25% reduction of SZE signals at $\nu = 353$ GHz. It is also noted that the ν value for the zero thermal SZE point depends on the gas temperature, in contrast with that of the nonrelativistic case (e.g., Birkinshaw 1999; Rephaeli 1995). As pointed out by Itoh et al. (1998), their perturbative approximation is valid up to $k_B T_{gas} = 15$ keV in comparison with that from exact numerical calculations. At $k_B T_{gas} \sim 20$ keV, the approximated result

deviates from the full numerical one significantly at $\nu > 500$ GHz. At $\nu \leq 353$ GHz, however, equation (2) is still a good approximation even for $k_B T_{gas} \sim 20$ keV.

Consider unresolved clusters, the total flux of the thermal SZE from a cluster at redshift z is

$$S = \frac{1}{R_d^2(z)} \int \Delta I dA, \quad (3)$$

where $R_d(z)$ is the angular diameter distance to the cluster, and the integral is over the surface area of the cluster.

With the isothermal assumption, equation (3) can be written as

$$S = I_0 \frac{x^4 e^x}{(e^x - 1)^2} (Y_0 + \theta_e Y_1 + \theta_e^2 Y_2 + \theta_e^3 Y_3 + \theta_e^4 Y_4) Y, \quad (4)$$

where

$$Y = \frac{1}{R_d^2} \int y dA. \quad (5)$$

If we denote f_b as the gas fraction that is assumed to be a constant and X as the hydrogen mass fraction, then

$$Y = \frac{\sigma_T}{2m_e m_p c^2} f_b (1 + X) k_B T_{gas} M R_d^{-2}, \quad (6)$$

where M is the total mass of the cluster, and m_p is the proton mass. Further under the equilibrium condition, the temperature T_{gas} and the mass M are related through the following relation (e.g., Wang & Steinhardt 1998)

$$k_B T_{gas} = 0.944 f_\beta (1 + z) [\Omega_m(0) \Delta_c]^{1/3} \times \left[1 - \frac{2\Omega_\Lambda(z)}{\Delta_c \Omega_m(z)} \right]^{-3/2} \left(\frac{M}{10^{15} h^{-1} M_\odot} \right)^{2/3}, \quad (7)$$

where $f_\beta = f_\mu \mu / \beta$ with f_μ a constant factor of order unity that reflects the deviation from the simple spherical model, μ the mean molecular weight of the gas, and β the ratio of the kinetic energy of galaxies to the thermal energy of the gas, $\Omega_m(z)$ and $\Omega_\Lambda(z)$ are the matter density parameter and the dark energy density parameter at redshift z , respectively, and Δ_c is the ratio of the mean density of the cluster to the background matter density at redshift z . Here μ is related to X by $\mu = 4/(5X + 3)$.

Then given a flux limit for a SZE survey, one can get the corresponding mass limit $M_{lim}(S_{lim}, z)$ from equations (4), (6) and (7). Note that the mass limit depends on cosmological models.

2.2. Cluster Number Densities and Cosmological Models

For the comoving number density of clusters, we use the fitting formula of Jenkins et al. (2001). Then we have

$$\frac{dn}{dM}(z, M) = 0.315 \frac{\rho_0}{M} \frac{1}{\sigma_M} \left| \frac{d\sigma_M}{dM} \right| \exp[-|0.61 - \ln(D_z \sigma_M)|^{3.8}], \quad (8)$$

where ρ_0 is the present matter density of the universe, σ_M is the rms of the linearly-extrapolated-to-present matter density fluctuation over the mass scale M , and D_z is the linear growth factor of density perturbations.

For σ_M , we adopt the form given by Viana & Liddle (1999)

$$\sigma_M = \sigma_8 \left[\frac{R(M)}{8h^{-1}\text{Mpc}} \right]^{-\gamma[R(M)]}, \quad (9)$$

where h is the Hubble constant in units of $100 \text{ km s}^{-1} \text{ Mpc}^{-1}$, the spatial scale R is related to M through

$$R(M) = \frac{M}{(4\pi/3)\rho_0},$$

and

$$\gamma(R) = (0.3\Gamma + 0.2) \left[2.92 + \log_{10} \left(\frac{R}{8h^{-1}\text{Mpc}} \right) \right], \quad (10)$$

with Γ the shape parameter of the linear density fluctuation spectrum.

In this paper, we consider flat cosmological models with the dark energy part described by the equation of state $w = p/\rho$. The density parameter of dark energy is then specifically denoted by Ω_Q . The linear growth factor D_z is given by the analytical formula of Wang & Steinhardt (1998)

$$D_z \approx a \exp \left\{ \int_a^1 \frac{da}{a} [1 - \Omega_m(z)^\alpha] \right\}, \quad (11)$$

where $a = 1/(1+z)$ is the scale factor of the universe, and

$$\alpha \approx \frac{3}{5-w/(1-w)} + \frac{3}{125} \frac{(1-w)(1-3w/2)}{(1-6w/5)^3} [1 - \Omega_m(z)].$$

For the over-density of a cluster collapsed and virialized at redshift z_c , we have (Wang & Steinhardt 1998)

$$\Delta_c(z_c) = \zeta \left(\frac{R_{ta}}{R_{vir}} \right)^3 \left(\frac{1+z_{ta}}{1+z_c} \right)^3, \quad (12)$$

where R_{ta} and R_{vir} are the radii of the cluster at the time of turn-around ($z = z_{ta}$) and at the time of virialization ($z = z_c$), respectively, and

$$\zeta = \frac{\rho_{cluster}(z_{ta})}{\rho_b(z_{ta})} \approx \left(\frac{3\pi}{4}\right)^2 \Omega_m^{-0.79+0.26\Omega_m-0.06w}|_{z_{ta}}. \quad (13)$$

The redshifts z_{ta} and z_c are related through $t(z_c) = 2t(z_{ta})$, i.e., the time at z_c is twice the turn-around time, and

$$\frac{R_{vir}}{R_{ta}} = \frac{1 - \eta_v/2}{2 + \eta_t - 3\eta_v/2}, \quad (14)$$

where

$$\eta_t = 2\zeta^{-1} \frac{\Omega_Q(z_{ta})}{\Omega_m(z_{ta})},$$

and

$$\eta_v = 2\zeta^{-1} \left(\frac{1 + z_c}{1 + z_{ta}}\right)^3 \frac{\Omega_Q(z_c)}{\Omega_m(z_c)}.$$

3. Results of Analyses

In the following studies, we take $f_b = 0.1$, $f_\beta = 1.4$, and $X = 0.76$ for the gas properties. For cosmological models, the Hubble constant H_0 is taken to be $70 \text{ kms}^{-1}\text{Mpc}^{-1}$, $\Omega_m(0) = 0.3$, and $\Omega_Q(0) = 0.7$. For perturbations, we take $\Gamma = 0.2$. The observational frequency is taken to be $\nu = 353 \text{ GHz}$.

3.1. Mass limits for Flux-limited SZE Surveys

From equations (4), (6), and (7), it is clear that the corresponding mass limit for a flux-limited SZE survey is cosmology-dependent, and this dependency is one of the factors that contribute to the differences of the expected SZE survey results for different cosmological models.

In Figure 2, we show M_{lim} , in units of $10^{15}h^{-1}M_\odot$, vs. redshift z for different w cosmologies given $S_{lim} = 30 \text{ mJy}$. The three models are for $w = -1$, $w = -0.75$, and $w = -0.3$, respectively. For each pair, the lower one is the result without relativistic corrections, and the upper one is the one with the effects included. It is seen that the mass limit decreases as w increases. At $z = 1$, $M_{lim}(w = -0.3) \approx 0.7M_{lim}(w = -1)$. The relative increase of the mass limit due to relativistic corrections ranges from 6.5% for $w = -1$ to 7.5% for $w = -0.3$ at $z = 1$.

3.2. SZE Cluster Number Counts

As flat models with different w have different volume elements, linear growth factors for density perturbations, and mass limits, the redshift distribution of SZE clusters is sensitive to w , and thus can be used to probe the w value.

In Figure 3a and Figure 3c, we show $dN/(d\Omega dz)$ for $S_{lim} = 5$ mJy and $S_{lim} = 30$ mJy, respectively, without relativistic corrections. In each figure, results of three models with $w = -1, -0.75$ and -0.3 are plotted. For all the models, $\sigma_8 = 0.85$. Therefore the figures show the effects of different w on the cluster redshift distribution. We see that given a flux limit, models with larger w (smaller absolute value of w) predict more SZE clusters over almost the whole redshift range considered. In Figure 3b and Figure 3d, relativistic corrections on $dN/(d\Omega dz)$ are shown. It is seen that they are larger at higher redshifts, and relatively smaller for higher w at redshifts $z \geq 1$. For $S_{lim} = 30$ mJy, the relative changes are about 13% at $z = 0.5$, and at $z = 2$, they are about 41%, 38% and 32% for $w = -1, -0.75$ and -0.3 , respectively.

In Figure 4, we show the surface number density $dN/d\Omega$ vs. w . For each pair, the upper and the lower ones are for the results without and with relativistic corrections, respectively. For $S_{lim} = 30$ mJy, the respective $dN/d\Omega = 1.45$ and 1.30 at $w = -0.75$, with the change of about 10%. For *Planck*, the survey area is about 10000 deg^2 . Then the corresponding 1σ uncertainty of $dN/d\Omega$ due to Poisson fluctuations is about 0.012 . Thus the change due to relativistic effects is about 12σ . This indicates the significance of the effects in extracting w value from observations. For example, with single-frequency measurements, given the observed surface number density of 1.30 , one would infer $w \approx 0.9$ if relativistic corrections are neglected, which is about 20% off the real value of $w = -0.75$. We elaborate this further in the next subsection.

In Figure 3 and Figure 4, $\sigma_8 = 0.85$ for all the models. That is, we assume that σ_8 , as well as other cosmological parameters, have been well determined from other observational information. On the other hand, studies have shown that the total number of SZE clusters is sensitive to σ_8 , thus potentially, σ_8 and w can be constrained from SZE surveys simultaneously. From the shape of the redshift distributions in Figure 3, we see that with the same total number of SZE clusters, the differences of the models are still apparent. For $S_{lim} = 5$ mJy, the number of clusters with $z \geq 1$ is significantly larger for larger w . The ratio $dN(z \geq 1, w = -0.3)/d\Omega$ to $dN(z \geq 1, w = -1)/d\Omega$ is about 1.8. For $S_{lim} = 30$ mJy, the number of clusters with $z \geq 0.5$ shows strong dependence on w , with $[dN(z \geq 0.5, w = -0.3)/d\Omega]/[dN(z \geq 0.5, w = -1)/d\Omega] \approx 1.8$. These analyses suggest that it is possible to constrain both σ_8 and w using the total number of SZE clusters and the number of SZE clusters with $z > z_m$ with z_m flux-limit dependent. With this methodology,

we only need to know the redshift range of a cluster, but not its precise z . Thus it is relatively easy to be realized in practice. In the next subsection, we show how well we can apply this method to constrain σ_8 and w . We also discuss relativistic effects on the parameter determination.

3.3. Constraints on σ_8 and w

We concentrate on extracting information on σ_8 and w from SZE cluster surveys by assuming that other cosmological parameters have been pre-determined. The values of those other parameters considered in this paper were listed at the beginning of Section 3.

Two pieces of information will be used to constrain σ_8 and w : the total number of SZE clusters and the number of clusters with $z \geq z_m$. Here we take $S_{lim} = 30$ mJy and $z_m = 0.5$.

The model with $\sigma_8 = 0.8284$ and $w = -0.75$ is adopted as the fiducial one. We choose $w = -0.75$ (but not $w = -1$) as our central value so that relativistic effects can be seen clearly (see Figure 6 in the following). Our analyzing procedures are as follows. Given the total surface number density $dN/d\Omega$ calculated from the fiducial model, we search for σ_8 for different w -models such that they have the same $dN/d\Omega$ as that of the given value. In this way, we get a relation between σ_8 and w . Similarly, there is another σ_8 - w relation from the number density of clusters with $z \geq 0.5$ [denoted as $dN(z \geq 0.5)/d\Omega$]. The two lines from the two relations should intersect at $\sigma_8 = 0.8284$ and $w = -0.75$. Given a survey area, we can estimate the possible constrained ranges for σ_8 and w allowing different uncertainty levels.

Figure 5 shows σ_8 - w relations for $S_{lim} = 30$ mJy without (thin lines) and with (thick lines) relativistic corrections. The set of relatively flat lines are from $dN/d\Omega$, and the other set of lines are from $dN(z \geq 0.5)/d\Omega$. The solid lines are from the fiducial $dN/d\Omega$ and $dN(z \geq 0.5)/d\Omega$, respectively. The dashed lines are $\pm 3\sigma$ results for $dN/d\Omega$, and the dotted lines are $\pm 3\sigma$ results for $dN(z \geq 0.5)/d\Omega$. Here Poisson statistics is applied to estimate σ , and the survey area is taken to be 10000 deg^2 .

For the non-relativistic case, we find that the solid lines can well be fitted by

$$\sigma_8(w) = 0.8284|w + 0.75 - 1|^{(0.1353 - 0.0150|w + 0.75 - 1|)}, \quad (15)$$

and

$$\sigma_8(w) = 0.8284|w + 0.75 - 1|^{(0.1809 - 0.0056|w + 0.75 - 1|)}. \quad (16)$$

To avoid crowding, we did not plot 1σ and 2σ lines in Figure 5. Our studies show that with 1σ uncertainties in both the total number of SZE clusters and the number of clusters with

$z \geq 0.5$, σ_8 and w are constrained to be within the ranges $(0.8209, 0.8360)$ and $(-0.81, -0.69)$, respectively. Thus for a survey such as *Planck*, the respective accuracies of the determined σ_8 and w can possibly reach to a level of about $\pm 1\%$ and $\pm 8\%$. The 3σ determinations are about $\pm 3\%$ for σ_8 and about $\pm 25\%$ for w if other cosmological parameters have already been known to good precisions.

In the relativistic case, the approximated analytical relations between σ_8 and w for the solid lines are

$$\sigma_8(w) = \sigma_8(-0.75)|w + 0.75 - 1|^{(0.1246 - 0.0115|w + 0.75 - 1|)}. \quad (17)$$

and

$$\sigma_8(w) = \sigma_8(-0.75)|w + 0.75 - 1|^{(0.16969 - 0.00009|w + 0.75 - 1|)}. \quad (18)$$

The relations are slightly flatter than those of the nonrelativistic case (eq. [15] and eq. [16]). As seen in Figure 3d, relativistic effects are stronger at higher redshifts. It is also known that models with larger w (lower absolute w value) predict more high redshift clusters, and thus the relativistic corrections to $dN/d\Omega$ and $dN(z \geq 0.5)/d\Omega$ are larger. This results the decrease of the differences between different w models in terms of the two measurements, and therefore the flatter σ_8 - w relations. The 1σ and 3σ ranges for σ_8 are $(0.8213, 0.8356)$ and $(0.8056, 0.8491)$, respectively, and the respective ranges for w are $(-0.815, -0.69)$ and $(-0.95, -0.57)$. We see that relativistic corrections do not affect the precisions of the parameter determination very much.

On the other hand, however, if relativistic effects were neglected in extracting σ_8 and w from a SZE survey, the determined central values can be significantly off the real ones. To estimate this misplacement, we take the relativistic $dN/d\Omega$ and $dN(z \geq 0.5)/d\Omega$ from the fiducial model with $\sigma_8 = 0.8284$ and $w = -0.75$ as inputs, but search for σ_8 - w relations with *nonrelativistic* mass limits. In Figure 6, we plot the results as solid lines. The contours are the 1σ (solid), 2σ (dotted) and 3σ (dashed) lines around $\sigma_8 = 0.8284$ and $w = -0.75$ (denoted by the star). Note that the solid contour is composed by $\pm 1\sigma$ lines for the total number of SZE clusters and the $\pm 1\sigma$ lines for the number of clusters with $z \geq 0.5$. The 2σ and 3σ contours are similar. First let us consider one parameter case (given the other) using the total number of SZE clusters as the constraint. Given $\sigma_8 = 0.8284$, the derived central w from the wrong solid line is $w \approx 0.92$, while the 3σ value is $w \approx 0.78$. On the other hand, if $w = -0.75$ is given, the derived σ_8 is $\sigma_8 \approx 0.814$, while the 3σ value is $\sigma_8 \approx 0.824$. We see that the misplacement is dramatically large. If both σ_8 and w are considered as unknown, the derived values from the cross-point of the two solid lines are $\sigma_8 \approx 0.819$ and $w \approx -0.81$. Thus the derivations from the fiducial values are about 1.1% for σ_8 and 8% for w . Although this offset is smaller than those of the one parameter cases, the derived "central values" are outside the 3σ region (the region surrounded by the dashed contour). Therefore relativistic

effects are very significant and cannot be ignored.

4. Discussion

As the most important property of SZE is its redshift-independence, SZE cluster surveys are one of the best to probe the structure formation at high redshifts. Because of the cosmological model dependence of the geometry of the universe, of the evolution of density fluctuations, and of the mass limit corresponding to a given flux limit, the redshift distribution of SZE clusters is sensitive to cosmological parameters.

We particularly discussed the effects of relativistic corrections of thermal SZE on the redshift distribution of clusters, and further on σ_8 and w determinations from SZE cluster surveys. The corrections affect the cluster redshift distribution through changing the mass limit for a given flux limit. The changes depend on the observing frequency and on the flux limit. For $\nu = 353$ GHz and $S_{lim} = 30$ mJy, at $z = 1$, the relative increase of the mass limit due to relativistic effects is about 6.5% and 7.5% for $w = -1$ and $w = -0.3$, respectively. With $\sigma_8 = 0.85$ for all the models, the corresponding decrease of $dN/d\Omega$ is about 8.9% and 13.5% for $w = -1$ and $w = -0.3$, respectively. For $dN(z \geq 0.5)/d\Omega$, the percentages of the decrease are, respectively, about 18.4% and 21.3% for $w = -1$ and $w = -0.3$.

With fixed other cosmological parameters, we studied the constraints on σ_8 and w from the total number of SZE clusters and from the number of clusters with $z \geq z_m$, where z_m is flux-limit dependent. For $S_{lim} = 5$ mJy, $z_m = 1.0$ is appropriate. For $S_{lim} = 30$ mJy, $z_m = 0.5$. The nice part of our methodology discussed here is that we do not need to know the precise redshift of a cluster, but only its range, i.e., larger or smaller than z_m . Therefore it is applicable in large surveys, such as *Planck*, because then one can use not-so-precise methods to estimate the redshifts of clusters, such as the photometric method or morphological redshift estimates (Diego et al. 2003). Our study showed that at $S_{lim} = 30$ mJy, for a survey of 10000 deg^2 , σ_8 can be determined to a level of $\pm 1\%$ and w to an accuracy of $\pm 8\%$ with 1σ uncertainties in both the total number of clusters and the number of high redshift clusters ($z \geq 0.5$ in our analyses). With 3σ uncertainties, the determined parameter ranges are $\pm 3\%$ and $\pm 25\%$ around the central values of σ_8 and w , respectively. In our uncertainty estimations in subsection 3.3, we assumed that the redshift information is available for 100% SZE clusters. That is, when we assessed the σ for the number of clusters with $z \geq 0.5$, we used the full number of clusters with $z \geq 0.5$ for a survey of 10000 deg^2 . If the redshifts are available for 10% of clusters, with 1σ uncertainties, the determined σ_8 and w have the ranges (0.815, 0.842) and $(-0.89, -0.62)$ around the central values $\sigma_8 = 0.8284$ and $w = -0.75$. Thus with 10% samples having redshift information, the accuracies of 1σ

determination for σ_8 and w are $\pm 1.6\%$ and $\pm 18\%$, respectively. Relativistic corrections do not have significant effects in this aspect.

However, we found that the central values of σ_8 and w can be significantly misplaced if relativistic corrections are not included in extracting cosmological information from observed cluster number counts. For $S_{lim} = 30$ mJy, the offset for σ_8 is about 1.1%, and about 8% for w . In terms of the percentages, this misplacement is comparable to the 1σ deviation. But the location of the wrong central values in the $\sigma_8 - w$ plane is significantly outside the 3σ region around the real central (σ_8, w) as seen in Figure 6. Therefore, relativistic effects are important, and should be considered carefully in analyzing survey results.

We need to emphasize that our discussions on relativistic effects concentrate on single-frequency measurements at 353 GHz. In reality, *Planck* will conduct multi-frequency observations, and the overall relativistic effects could be weaker than the case of $\nu = 353$ GHz depending on the techniques used to detect SZE clusters. Diego, Hansen & Silk (2003) studied the impact of relativistic corrections on the reconstruction of the y map from simulated $\Delta T/T$ of different frequency channels with Bayesian non-parametric method. They found that for clusters of $T = 10$ keV, the relative difference in the recovered y between relativistic and non-relativistic approaches in the component separation was about 4% for low-redshift clusters and about 8% for high-redshift clusters. This difference is smaller than that at $\nu = 353$ GHz, which is about 15%. This is because the y maps were constructed through the weighted average of $\Delta T/T$ of different frequency channels, and relativistic corrections are smaller than 10% for $\nu < 353$ GHz. Thus the single-frequency estimation of relativistic effects presented in this paper can be an over-estimation. To quantify the impact realistically, one can, with simulated maps including characteristics of a survey, get two sets of mass limits of detectable SZE clusters at different redshifts with and without relativistic corrections for a particular cosmological model. Then analytical studies similar to those shown in this paper can be carried out based on the two sets of mass limits. We would like to mention that the flux limit for completeness, thus the mass limit, depends on the method applied to find clusters. The limit $S_{lim} = 30$ mJy (at $\nu = 353$ GHz) adopted in our analyses is from the estimation of Diego et al. (2002) based on the Maximum Entropy Method (Hobson et al. 1998; Hobson et al. 1999). On the other hand, Bayesian non-parametric method gives the completeness limit $S_{lim} \sim 200$ mJy (at $\nu = 353$ GHz) (Diego et al. 2003), and a multi-filter approach of Herranz et al. (2002) finds $S_{lim} \sim 170$ mJy. With such high flux limits, relativistic corrections can be large even with the multi-frequency diminishing effect taken into account.

The constraints on σ_8 and w shown in the paper are derived under the assumption that all other cosmological parameters have been determined by other studies. If we allow, e.g.,

$\Omega_m(0)$, to vary as well, the estimation can be affected considerably (e.g., Haiman, Holder, & Mohr 2001). On the other hand, however, there are indeed different types of observations that can give good constraints on those parameters. For example, galaxy surveys, such as two degree field Galaxy Redshift Survey (2dFGRS) (Colless et al. 2001) and the Sloan Digital Sky Survey (SDSS), can put constraints on the shape of the perturbation spectrum, which primarily depends on $\Omega_m h$ (Szalay et al. 2001; Dodelson et al. 2002; Percival et al. 2001; 2002). Combined with the measurements on the Hubble constant H_0 , Ω_m can be well constrained. In any case, studies on the multiple-parameter estimation with the methodology put forward in this paper and on the impact of relativistic corrections are desired, and will be carried in the future.

We thank the referee for the helpful comments and suggestions. This research was supported in part by the National Science Foundation of China under grant 10243006, and by the Ministry of Science and Technology of China under grant TG1999075401.

REFERENCES

- Bahcall, N., & Fan, X. 1998, *ApJ*, 504, 1
- Birkinshaw, B. 1999, *Physics Report*, 310, 97
- Caldwell, R. R., Dave, R., & Steinhardt, P. J. 1998, *Ap&SS*, 261, 303
- Carlstrom, J. E., Holder, G. P., & Reese, E. D., 2002, *ARA&A*, 40, 643
- Diego, J. M., Martinez-Gonzalez, E., Sanz, J. L., Benitez, N., & Silk, J. 2002, *MNRAS*, 331, 556
- Diego, J. M., Hansen, S. H., & Silk, J. 2003, *MNRAS*, 338, 796
- Diego, J. M., Mohr, J., Silk, J., & Bryan, G. 2003, *MNRAS*, 341, 599
- Dodelson, S. et al. 2002, *ApJ*, 572, 140
- Eisenstein, D. J., Hu, W., & Tegmark, M. 1999, *ApJ*, 518, 2
- Fan, Z. H., & Chiueh, T. H. 2001, *ApJ*, 550, 547
- Haiman, Z., Mohr, J. J., & Holder, G. P. 2001, *ApJ*, 553, 545

- Herranz, D., Sanz, J. L., Hobson, M. P., Barreiro, R. B., Diego, J. M., Martnez-Gonzalez, E., Lasenby, A. N. 2002, MNRAS, 336, 1057
- Hobson, M. P., Jones, A. W., Lasenby, A. N., Bouchet, F. R. 1998, MNRAS, 300, 1
- Hobson, M. P., Barreiro, R. B., Toffolatti, L., Lasenby, A. N., Sanz, J., Jones, A. W., Bouchet, F. R. 1999, MNRAS, 306, 232
- Holder, G., Haiman, Z., & Mohr, J. J. 2001, ApJ, 560, L111
- Itoh, N., Kohyama, Y., & Nozawa, S. 1998, ApJ, 502, 7
- Jenkins, A. et al. 2001, MNRAS, 321, 372
- Majumdar, S., & Mohr, J.J. 2003, ApJ, 585, 603
- Mohr, J. J., O’Shea, B., Evrard, A. E., Bialek, J., & Haiman, Z. 2002, astro-ph/02028102
- Pen, U. L. 1998, ApJ, 498, 60
- Percival, W. J. et al. 2001, MNRAS, 327, 1297
- Percival, W. J. et al. 2002, MNRAS, 337, 1068
- Perlmutter, S. et al. 1999, ApJ, 517, 565
- Pointecouteau, E. et al. 1999, ApJ, 519, L115
- Pointecouteau, E. et al. 2001, ApJ, 552, 42
- Rephaeli, Y., 2002, Space Science Reviews, 100, 61
- Rosati, P., Borgani, S., & Norman, C. 2002, ARA&A, 40, 539
- Schmidt, B. P. et al. 1998, ApJ, 507, 46
- Spergel, D. N. 2003, astro-ph/0302209
- Sunyaev, R. A., & Zel’dovich, Ya. B. 1980, ARA&A, 18, 537
- Szalay, A. et al. 2001, astro-ph/0107419
- Viana, P. T. P., & Liddle, A. R. 1999, MNRAS, 303, 535
- Wang, L., & Steinhardt 1998 ApJ, 508, 483

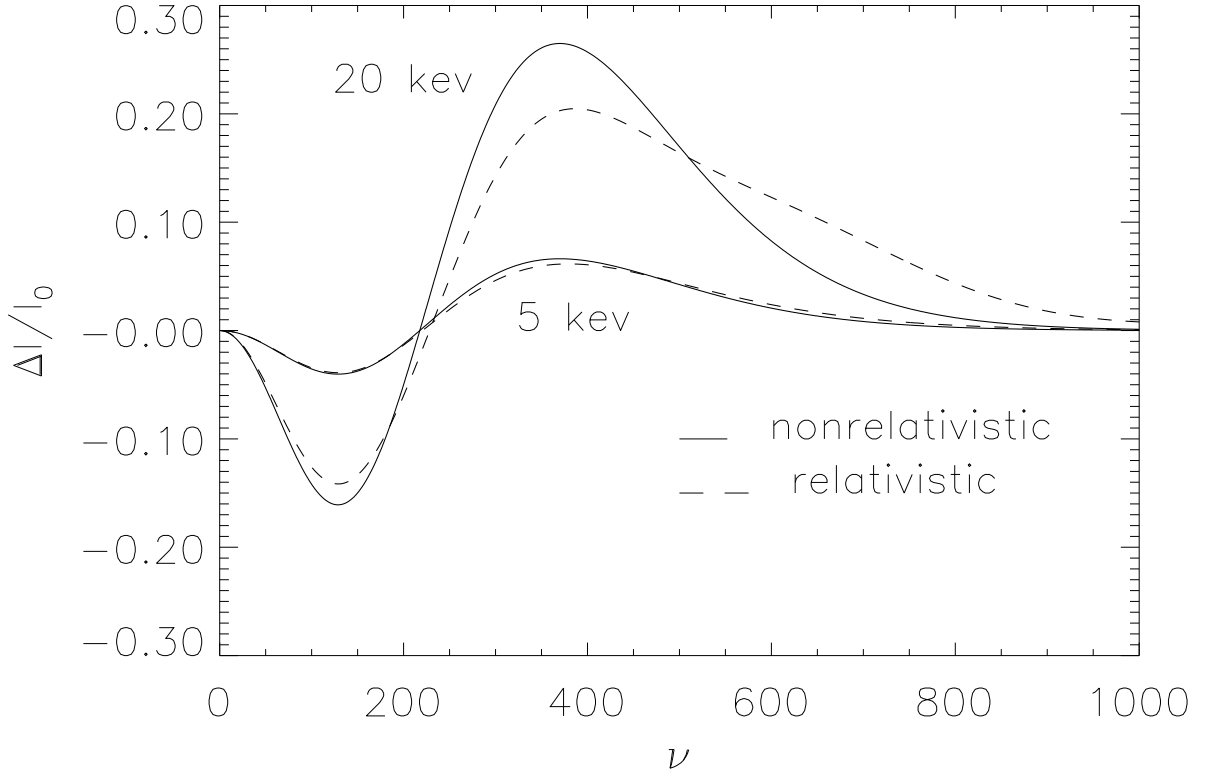


Fig. 1.— Thermal SZE $\Delta I/I_0$ after a single scattering with $I_0 = (2h_p/c^2)(k_B T_{CMB})^3/h_p^3$ vs. frequency ν for $k_B T_{gas} = 5$ keV and 20 keV. In each pair, the solid line represents the result without relativistic corrections, and the dashed line is for the results with relativistic corrections up to $(k_B T_{gas}/m_e c^2)^5$.

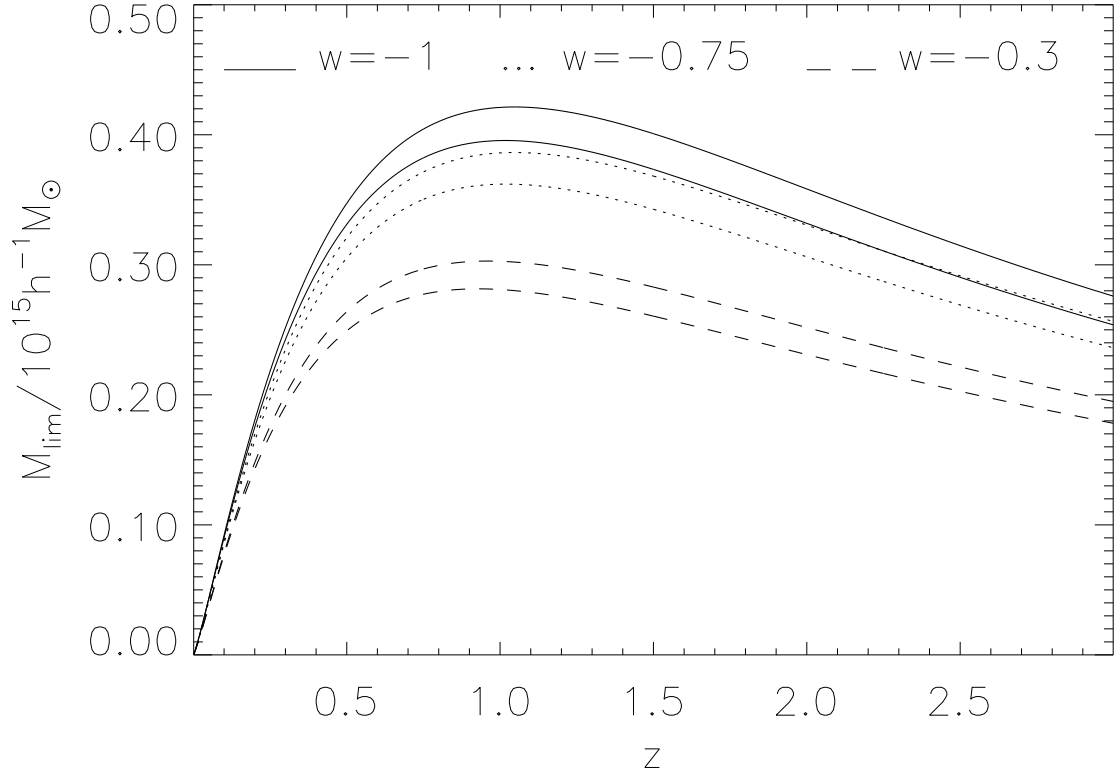


Fig. 2.— The mass limit M_{lim} in units of $10^{15} h^{-1} M_{\odot}$ vs. redshift z . The flux limit is $S_{lim} = 30$ mJy. The solid lines are for $w = -1$, the dotted lines are for $w = -0.75$ and the dashed lines are for $w = -0.3$. In each pair, the upper one corresponds to the one with relativistic corrections included, and the lower one is for nonrelativistic M_{lim} .

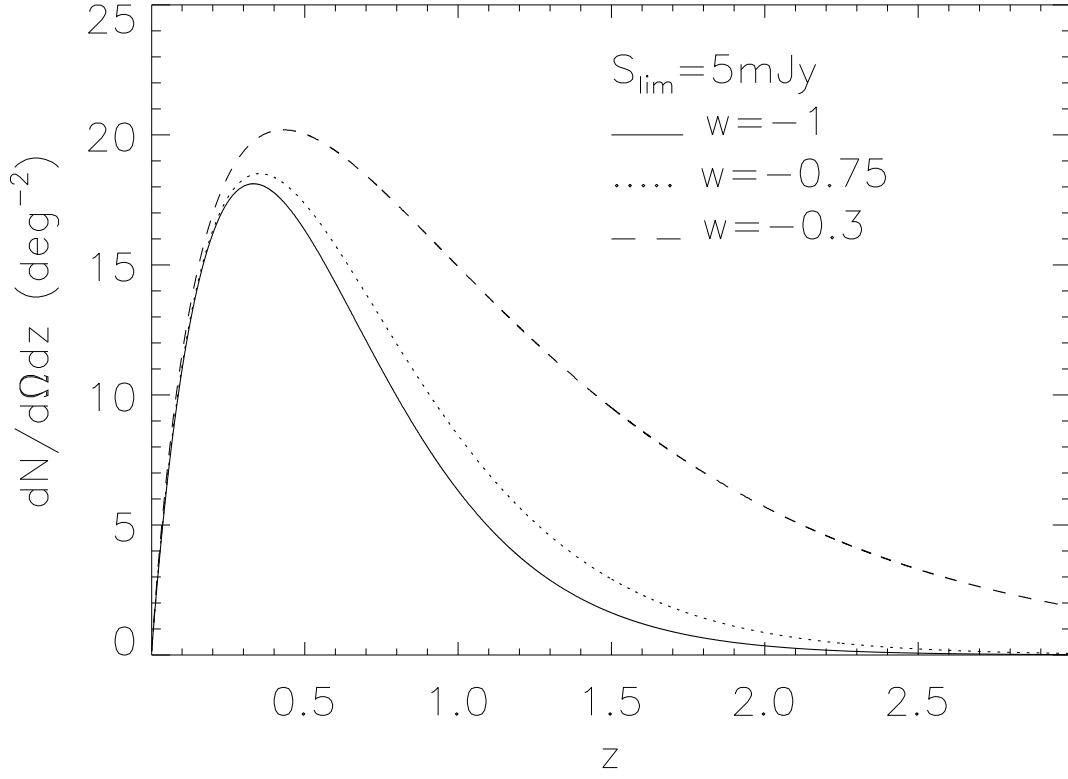


Fig. 3.— The redshift distribution of SZE clusters $dN/(d\Omega dz)$ in units of deg^{-2} for $S_{\text{lim}} = 5 \text{ mJy}$. No relativistic corrections are included, and $\sigma_8 = 0.85$. The solid line is for $w = -1$, the dotted line is for $w = -0.75$, and the dashed line is for $w = -0.3$.

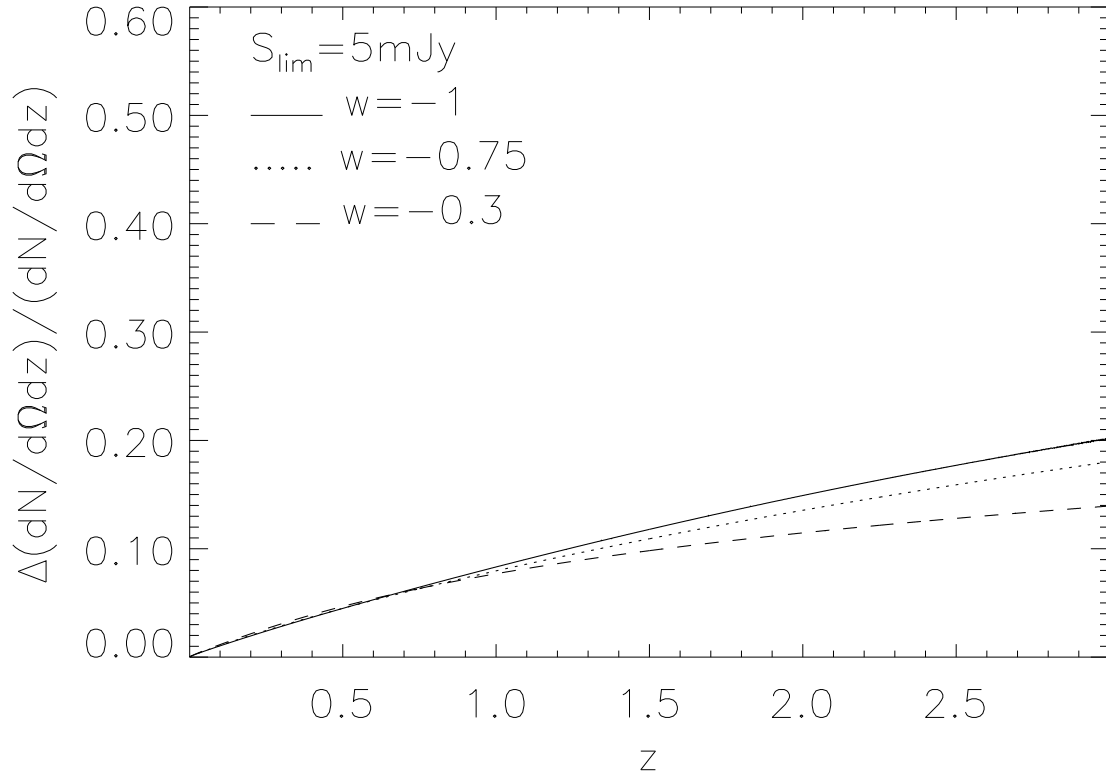


Fig. 4.— Relative changes of the redshift distribution of SZE clusters due to relativistic corrections for $S_{lim} = 5 \text{ mJy}$ and $\sigma_8 = 0.85$.

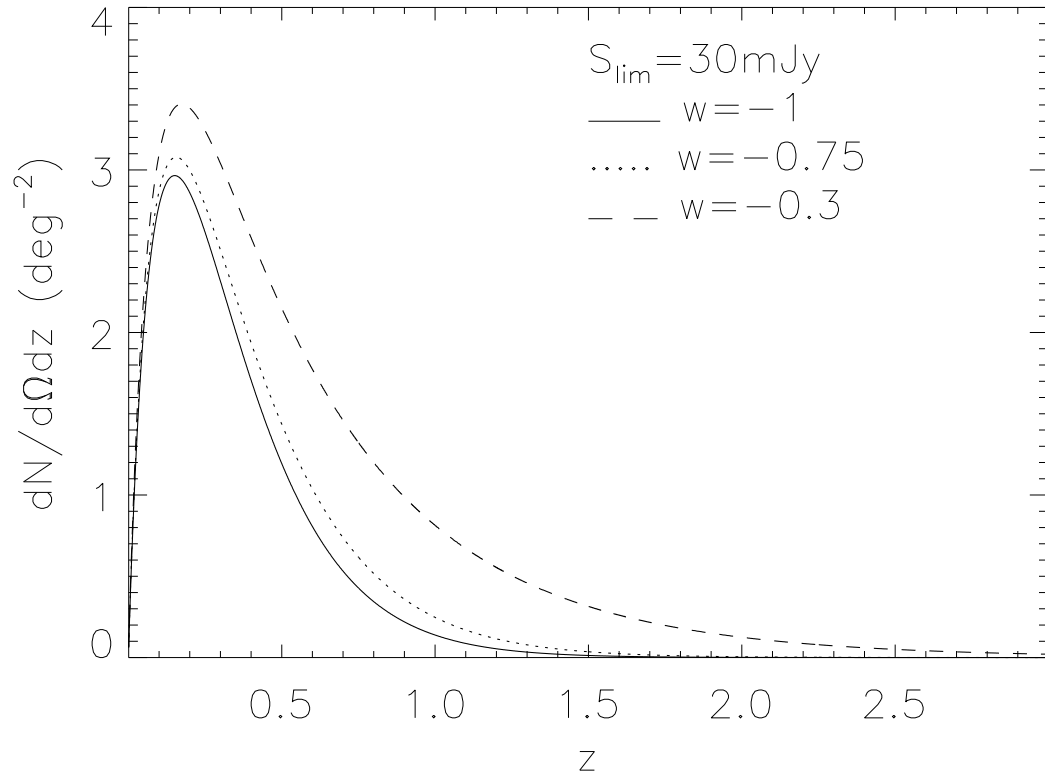


Fig. 5.— Same as fig.3a but for $S_{\text{lim}} = 30 \text{ mJy}$

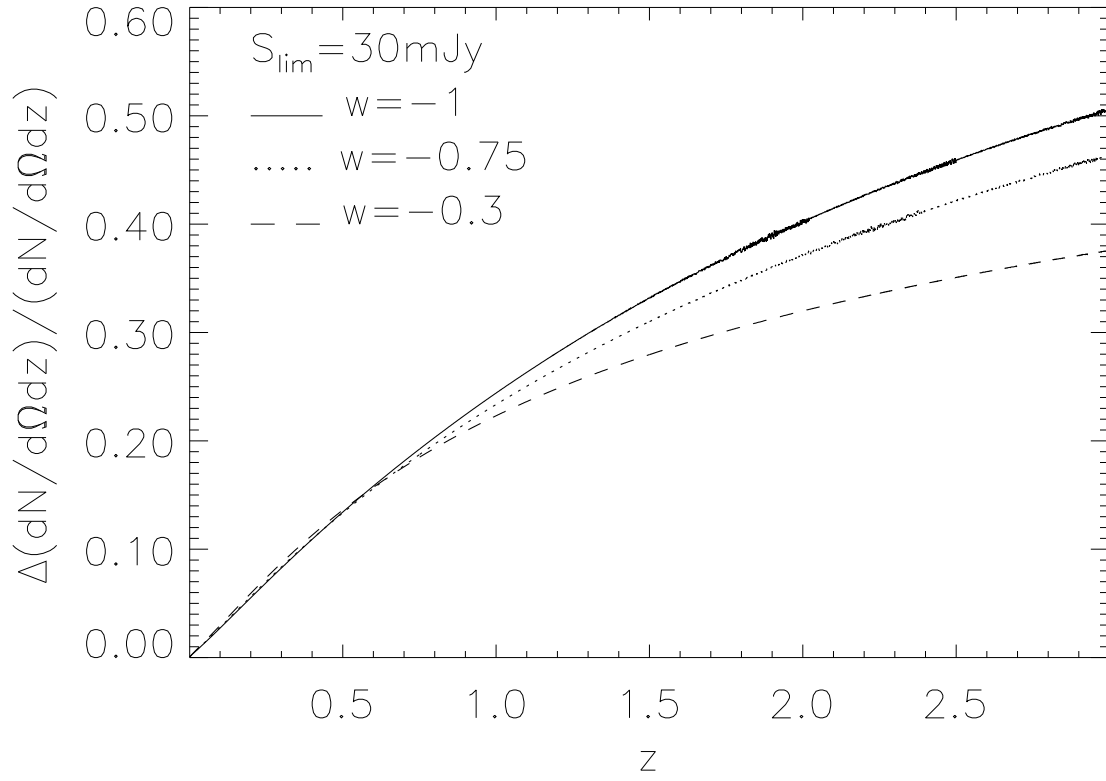


Fig. 6.— Same as fig.3b but for $S_{lim} = 30 \text{ mJy}$

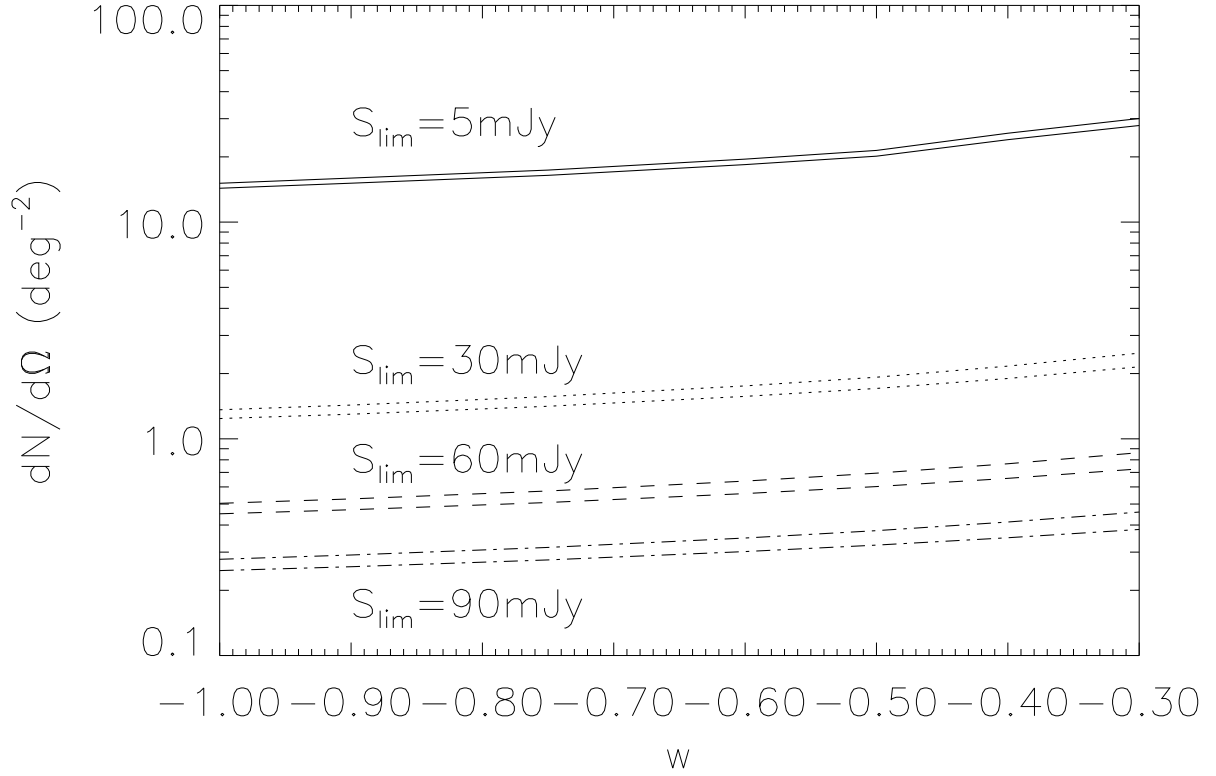


Fig. 7.— The surface number density of SZE cluster $dN/d\Omega$ in units of deg^{-2} vs. w . The solid, dotted, dashed and dash-dotted lines are for $S_{lim} = 5$ mJy, 30 mJy, 60 mJy and 90 mJy, respectively. In each pair, the upper one is the nonrelativistic result, and the lower one is the result with relativistic corrections included. Here $\sigma_8 = 0.85$ for all the models.

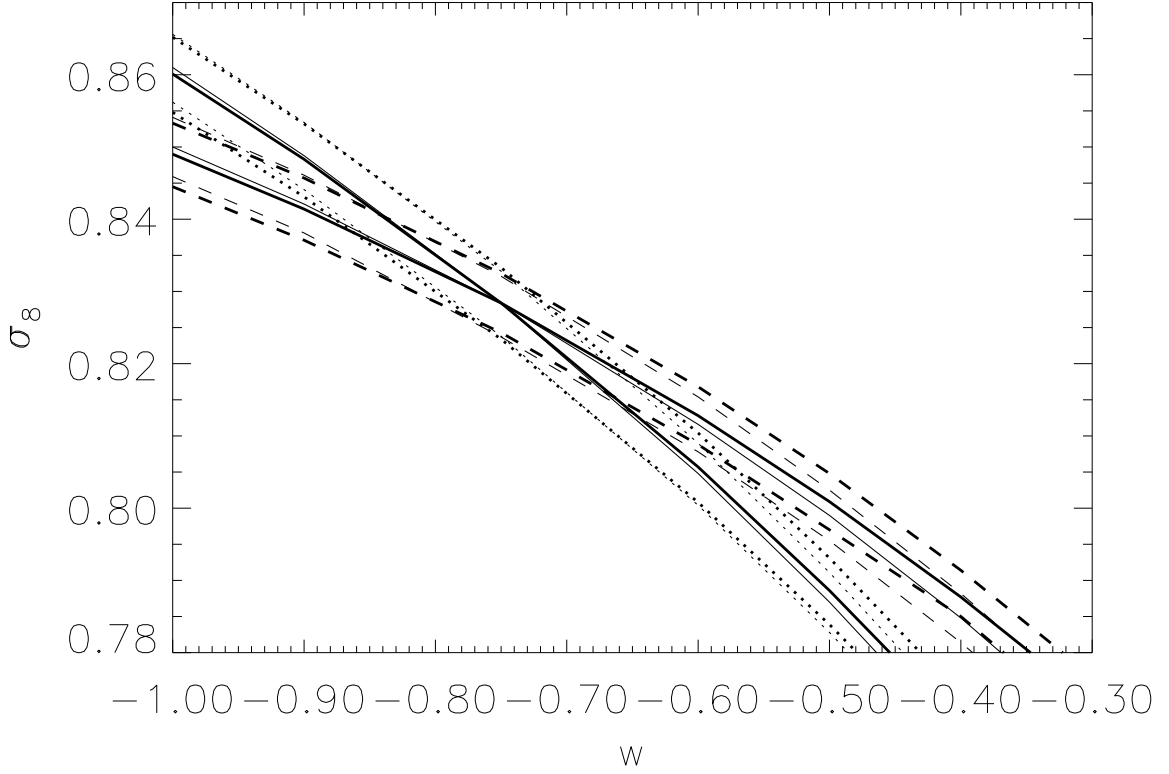


Fig. 8.— The $\sigma_8 - w$ relations without (thin lines) and with (thick lines) relativistic corrections. The set of relatively flatter lines are from the total number of SZE clusters, and the steeper lines are from the number of clusters with $z \geq 0.5$. The solid lines are from the central values of N_{tot} and $N_{z \geq 0.5}$, respectively. The dashed lines are the $\sigma_8 - w$ relations from $N_{tot} \pm 3\sigma$, respectively, and the dotted lines are the respective relations from $N_{z \geq 0.5} \pm 3\sigma$. The survey area is taken to be 10000 deg^2 .

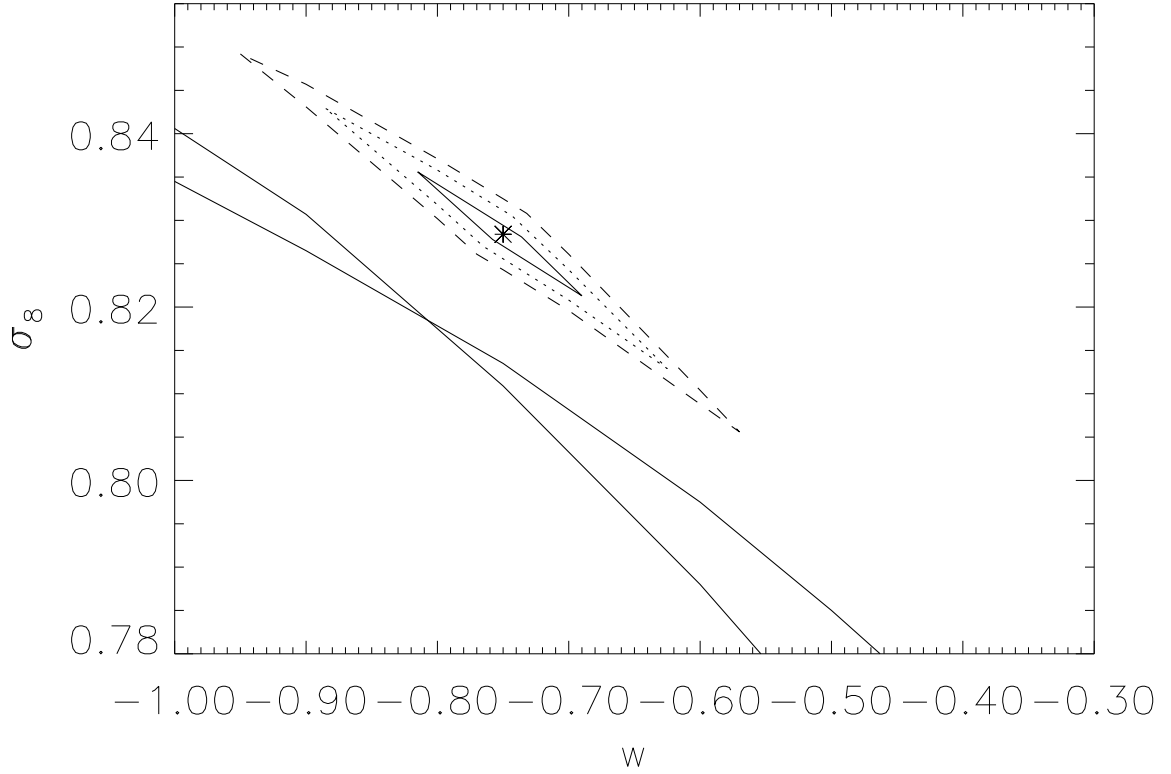


Fig. 9.— The misplacement of the central σ_8 and w . The two solid lines are from the nonrelativistic calculations given N_{tot} and $N_{z \geq 0.5}$ calculated relativistically with $w = -0.75$ and $\sigma_8 = 0.8284$ (represented by the star in the figure). The survey area is taken to be 10000 deg^2 . The solid, dotted, and dashed closed lines are 1σ , 2σ and 3σ deviations around $w = -0.75$ and $\sigma_8 = 0.8284$ (see the text for details).